Structure and electrochemistry of $Li_xMo_6S_8$

W. R. McKinnon and J. R. Dahn

Solid State Chemistry, National Research Council of Canada, Ottawa, Ontario, Canada K1A 0R9

The Chevrel compound $Li_xMo_6S_8$ has four phases for $0 < x < 1$: two rhombohedral phases, a rhombohedral phase with an incommensurate lattice distortion, and a triclinic phase. The lattice parameters in each phase have been measured, and the transitions between the phases have been studied with the use of intercalation batteries.

I. INTRODUCTION

Lithium Chevrel compounds can be prepared in electrochemical cells.[1-4] We recently reported the structure and electrochemistry of $Li_xMo_6Se_8$,[4] and showed that there are three structural transitions as x changes. Here we report the structure and electrochemistry of $Li_xMo_6S_8$ for $0 < x < 4$. We find a first-order transition from $x = 1$ to 3 between rhombohedral structures, and a transition from a rhombohedral structure near $x = 3.8$ to a triclinic structure near $x = 4$. This latter transition occurs in two steps; the intermediate phase has an incommensurate lattice distortion with a wave vector that varies with x.

Section II describes our experimental methods. Section III presents the electrochemistry and the structure of $Li_xMo_6S_8$. Section IV discusses the results near $x = 4$.

II. EXPERIMENTAL TECHNIQUES

From $Cu_3Mo_6S_8$ prepared by reacting Cu_2S, Mo, and MoS_2 in sealed quartz tubes at 1150°C for 65 h, we prepared Mo_6S_8 by leaching out the Cu in a solution of iodine and acetonitrile.[2] Electrochemical cells were made both from Mo_6S_8 and from $Cu_3Mo_6S_8$ as described by Dahn and Haering.[5] In $Li/Li_xCu_3Mo_6S_8$ cells, the Cu comes out of the Mo_6S_8 host when the cell is discharged[2,3,6] and after several cycles it no longer goes back into the host when the cell is charged.[6] Thus $Li_xMo_6S_8$ can be studied in cells made with either Mo_6S_8 or $Cu_3Mo_6S_8$ and we obtained the same results in both cases. These cells were charged and discharged with a constant current as described elsewhere.[7] Cells for *in situ* x-ray diffraction were assembled as described by Dahn *et al.*[8] These cells were held at constant voltages to prepare samples close to equilibrium, then the x-ray diffraction spectrum was taken. The x-ray cells were also cycled with a constant current while x-ray spectra were being continuously recorded, so that the structural distortion near $x = 4$ could be studied in more detail.

III. EXPERIMENTAL RESULTS

Figure 1 shows the voltage of a $Li/Li_xMo_6S_8$ electrochemical cell as a function of x at 28°C. The data are similar to those reported elsewhere.[1-3] The values of x have been normalized to $x = 0$ at 2.7 V and $x = 4$ at 1.75 V. Figure 2 shows $-dx/dV$ versus V in this range of x. There are peaks in $-dx/dV$ near 2.45, 2.08, and 1.8 V. Figure 3 shows the voltage range near $x = 4$ in more detail; there are two peaks, at 1.81 and 1.83 V.

Peaks in $-dx/dV$ can indicate phase transitions in intercalation compounds;[9] here they all do except the peak at 2.45 V. The nature of the transition can sometimes be inferred from the shift between charge and discharge in
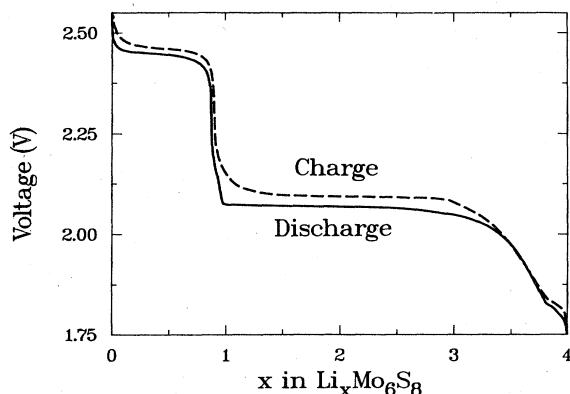

FIG. 1. Voltage V versus x of a $Li/Li_xMo_6S_8$ cell charging (— — —) and discharging (———) at a 12.5-h rate. (A 12.5-h rate corresponds to the current needed to change x by $\Delta x = 1$ in 12.5 h.) The data are normalized to $x = 0$ at 2.6 V and $x = 4$ at 1.75 V.
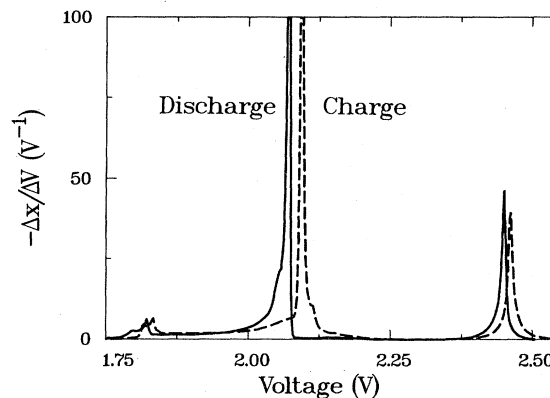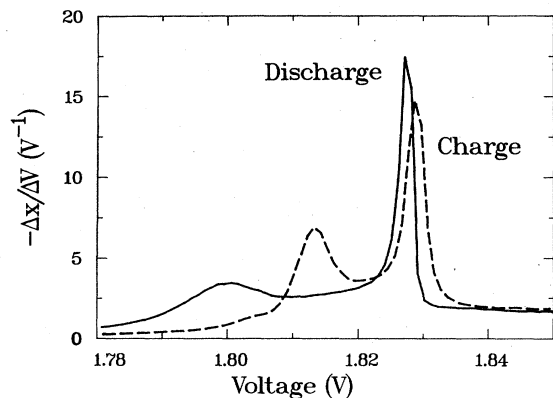

FIG. 2. $-dx/dV$ versus x from Fig. 1.

FIG. 3. $-dx/dV$ versus V for $3.6 < x < 4$ from a Li/Li$_x$Mo$_6$S$_8$ cell charging (— — —) and discharging (———) at a 200-h rate. The peak at higher voltage corresponds to the transition from R_2 to I and that at lower voltages to the transition from I to T. The data have been normalized as described in the text.

the voltage of the peak at small currents; this shift is usually smaller for a continuous transition than for a first-order one. Part of this shift in voltage is caused by losses such as resistance, but in first-order transitions there is an extra contribution from hysteresis in the transition. Figures 2 and 3 suggest that the peaks at 2.08 and 1.81 V are first-order transitions but that the peak at 1.83 V is a continuous transition; our x-ray studies support this.

Figure 4 shows the lattice parameters as a function of x, obtained by fixing the voltage of cells as described in Sec. II. There are four phases: two rhombohedral phases,
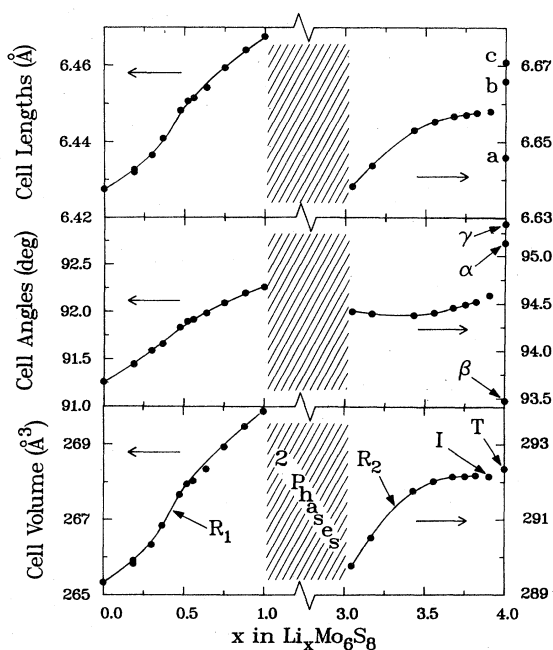

FIG. 4. Lengths, angles, and volume of the unit cell of Li$_x$Mo$_6$S$_8$ for the four phases R_1, R_2, I, and T. The solid lines, guides to the eye, join points in the same phase.

TABLE I. Summary of the phases of Li$_x$Mo$_6$S$_8$ and Li$_x$Mo$_6$Se$_8$. R represents rhombohedral, T represents triclinic, I represents rhombohedral with an incommensurate distortion.

Li$_x$Mo$_6$S$_8$		Li$_x$Mo$_6$Se$_8$	
$0 < x < 1$	R_1	$0 < x < 1$	R_1
$3 < x < 3.8$	R_2	$2.5 < x < 2.6$	T_1
$3.8 < x < 3.9$	I	$2.7 < x < 3.5$	R_2
$3.95 < x < 4$	T	$3.7 < x < 4$	T_2

R_1 and R_2; a rhombohedral phase with an incommensurate lattice distortion, I; and a triclinic phase, T. The lattice parameters agree with those reported by Tarascon et al.[2] at $x = 1.0$, 3.0, and 3.3. Tables I and II summarize the phases and the phase transitions in Li$_x$Mo$_6$S$_8$.

Between $x = 0$ and $x = 1$ the parameters vary smoothly with x, suggesting the material is a single phase. The volume, however, is not linear with x as it is in Li$_x$Mo$_6$Se$_8$.[10] The results in Fig. 2 for $x < 1$ may not be equilibrium results. In Li$_x$Mo$_6$S$_8$ for $x < 1$, cells discharged at constant current show broad Bragg peaks, and the lattice parameters as determined from the maxima of these peaks depend on the cell current. Moreover, $-dx/dV$ depends on the current and also differs from cell to cell. In Li$_x$Mo$_6$Se$_8$ the single phase below $x = 1$ is expected to form two phases near $x = 0.5$ below $-10°C$;[10] if that critical temperature for Li$_x$Mo$_6$S$_8$ is closer to room temperature, then the kinetics may slow near $x = 0.5$, a phenomenon known as critical slowing down.[11] We leave further discussion of the range of x from 0 to 1, which we call the R_1 phase, for a later publication.

Between $x = 1$ and $x = 3$ there is a first-order transition in which the R_1 phase coexists with a second rhombohedral phase R_2. In contrast, in Li$_x$Mo$_6$Se$_8$ the first-order transition which begins from the R_1 phase at $x = 1$ ends at $x = 2.5$ in a triclinic phase. Moreover, in Li$_x$Mo$_6$Se$_8$, $-dx/dV$ shows a small peak near $x = 2.6$, associated with the transition from this triclinic phase to the rhombohedral phase R_2. There is no such peak in Li$_x$Mo$_6$S$_8$.

For $3.8 < x < 4$ there are two peaks in $-dx/dV$ in Fig. 3, implying two phase transitions. The transition at higher voltage, which occurs near $x = 3.7$, shows little difference between the voltage of the peak on charge and discharge, and so may be continuous. At this transition, Li$_x$Mo$_6$S$_8$ changes from the R_2 phase to a phase I, a rhombohedral structure which has an incommensurate distortion. We obtained the lattice parameters in Fig. 2 for phase I by ignoring the satellite peaks in the x-ray spectrum. The transition at low voltage, which occurs

TABLE II. Summary of the phase transitions in Li$_x$Mo$_6$S$_8$ and Li$_x$Mo$_6$Se$_8$. F represents first order, C represents continuous.

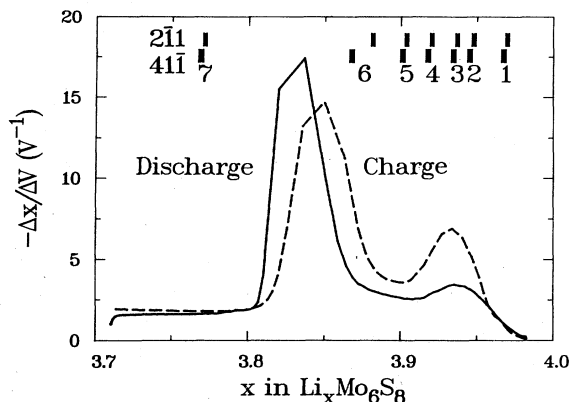| Li$_x$Mo$_6$S$_8$		Li$_x$Mo$_6$Se$_8$	
$R_1 \leftrightarrow R_2$	F	$R_1 \leftrightarrow T_1$	F
$R_2 \leftrightarrow I$	C?	$T_1 \leftrightarrow R_2$	F
$I \leftrightarrow T$	F	$R_2 \leftrightarrow T_2$	C?

FIG. 5. $-dx/dV$ from Fig. 4 versus x. The bars at the top of the figure indicate the range of x covered during each of the seven x-ray scans in Figs. 6 and 7.

near $x=3.9$, shows considerable hysteresis, suggesting a first-order phase transition. This is confirmed by the x-ray results (see Figs. 6 and 7 below) which show the coexistence of phase I with a triclinic phase T. The I phase is not seen in $Li_xMo_6Se_8$, although the Bragg peaks broaden when the triclinic phase at $x=4$ first begins to appear. The triclinic phase was indexed as described elsewhere,[4] and the fit obtained was as good as those reported there. The magnitude of the triclinic distortion in the T phase is about half as large as in the triclinic phase at $x=4$ in $Li_xMo_6Se_8$.[4]

Figure 5 shows $-dx/dV$ from Fig. 4 plotted versus x. The values of x were obtained as follows. From cells normalized to $x=0$ and 4 as in Fig. 1, the value of x at the larger peak in Fig. 4 was determined to be at $x=3.85$. The charge in Fig. 5 was then normalized to this value of
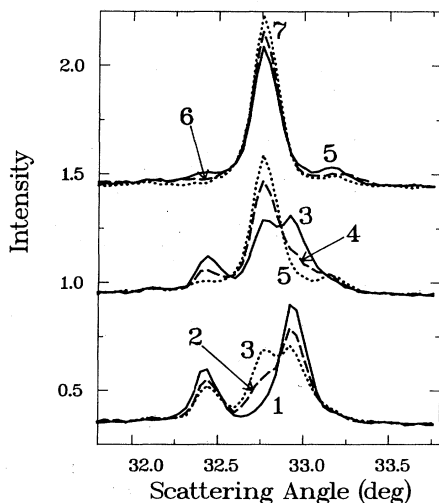

FIG. 6. X-ray diffraction spectrum near the $(2\bar{1}1)$ peak of R_2. The seven curves correspond to x shown in Fig. 5. In the T phase (curve 1), the peak at lower angle is $(2\bar{1}1)$, and that at higher angle is a combination of $(12\bar{1})$ and $(1\bar{1}\bar{2})$.
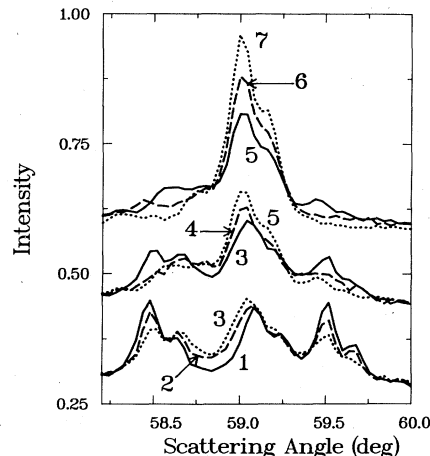

FIG. 7. As Fig. 6, near the $(41\bar{1})$ peak of R_2. Starting from low angle, the three peaks in phase T (curve 1) are $(1\bar{1}4)$, $(1\bar{4}\bar{1})$, and $(41\bar{1})$.

x at the peak and to $x=4$ at the lowest voltage. The subsequent discharge, which was over the same voltage range, was normalized to the same range of x as the charge. Such a procedure is necessary because side reactions at lower voltages make the charge transferred during discharge larger than during charge. This normalization may give large systematic errors in x, because it is based on the assumption that x goes to 4 in $Li_xMo_6S_8$. Differences in x, however, have little error. Note that the two peaks in $-dx/dV$ in Fig. 5 extend over the same range of x on charge and discharge, despite the hysteresis in Fig. 3.

Figures 6 and 7 show the evolution of two regions of the x-ray diffraction profile during the transitions from the R_2 through the I to the T phases. The values of x for the spectra are indicated in Fig. 5. Figure 6 shows the $(2\bar{1}1)$ peak in the R_2 phase, which splits into $(2\bar{1}1)$, $(12\bar{1})$, and $(1\bar{1}\bar{2})$ in the T phase. Figure 7 shows the $(41\bar{1})$ peak in the R_2 phase, which splits into $(1\bar{1}4)$, $(1\bar{4}\bar{1})$, and $(41\bar{1})$ peaks in the T phase. Note the satellites near the peak in the I phase. As x increases, these satellites move closer to the main peak and grow while the parent peak shrinks. When x reaches the lower peak in $-dx/dV$, both the parent peak and the satellites shrink while the triclinic peaks grow. The presence of these two sets of peaks shows that the transition from I to T is a first-order transition. On the other hand, because the satellite peaks are so small at lower x, we cannot tell whether they appear smoothly in a continuous transition or abruptly in a first-order one. Based on $-dx/dV$ in Fig. 3, we believe the transition from R_2 to I is continuous.

IV. PHASES NEAR $x=4$

In the (incommensurate) I phase, each Bragg peak except peaks of the form (hhh) in rhombohedral coordinates [or $(00h)$ in hexagonal coordinates] develops a pair of satellite peaks, one on each side of the parent peak. The satellites are close to their parent peaks, so the distortion has a long wavelength (the wave vector Q of the distortion

is near the center of the Brillouin zone). The transitions from R_2 to I phase and from I to T phase with x show analogies with the incommensurate transition in quartz. In quartz, the incommensurate phase appears in a continuous transition as the high-temperature β phase cools. The wavelength of the distortion increases from about 125 to 250 Å (Ref. 12) before the incommensurate phase disappears in a first-order phase transition to a low-temperature α phase. Thus, increasing x in $Li_xMo_6S_8$ has similar effects to decreasing T in quartz. $NaNO_2$ also has an incommensurate phase[13] with a wavelength which decreases with temperature, between about 29 and 35 Å. In both quartz and $NaNO_2$, Q is along the [100] direction in hexagonal coordinates [$(2\bar{1}\bar{1})$ in rhombohedral coordinates]. Such a distortion is also consistent with our results owing to the missing satellites for (hhh) peaks. Assuming such a distortion gives a wavelength of 180 ± 20 Å near the transition from I to T.

The equal intensities of peaks such as the ($1\bar{1}4$), ($1\bar{4}\bar{1}$), and ($41\bar{1}$) in Fig. 7 suggest that the relative positions of Mo and S atoms do not change much between R_2 and T phases. Since lithium scatters x rays only weakly, however, we can only infer the positions of the lithium atoms by analogy with other Chevrel compounds. When the rhom-

bohedral angle is larger than about 93°, there are two types of sites occupied by guest atoms:[14] type-1 sites, which form a hexagon around the origin of each unit cell, and type-2 sites, a pair of which appears between each hexagon of type-1 sites. Which of these sites the guest atoms occupy in triclinic phases is known only for $x < 2$. In the Cu and Fe Chevrel compounds, the intercalated atoms occupy two of the six type-1 sites in each hexagon at $x = 2$.[15,16] The two occupied sites are opposite one another on the hexagon, presumably to maximize the distance between Li atoms, and the same pair is occupied in each unit cell. For $x > 2$, some of the intercalated atoms are presumably in type-2 sites, as they are in the rhombohedral form of $Cu_xMo_6S_8$ with $x > 2$.[15] We can explain the limit $x=4$ in $Li_xMo_6S_8$ with the following assumptions: The same type-1 sites are occupied as in the triclinic phases of $Cu_2Mo_6S_8$ and $Fe_2Mo_6S_8$; the occupied type-2 sites are adjacent to empty type-1 sites; and only one of each pair of type-2 sites is occupied. If the lithium chooses the occupied type-2 site in each pair at random, this ordered structure gives no doubling of the axes of the unit cell in the triclinic phase, as observed. Alternatively, the limit $x=4$ might be set by the electron band structure.[17]

[1]R. Schollhorn, M. Kumpers, and J. O. Besenhard, Mater. Res. Bull. **12**, 781 (1977).

[2]J. M. Tarascon, F. J. DiSalvo, D. W. Murphy, G. W. Hull, and J. V. Waszczak (unpublished).

[3]P. J. Mulhern and R. R. Haering, Can. J. Phys. **62**, 527 (1984).

[4]J. R. Dahn, W. R. McKinnon, and S. T. Coleman, Phys. Rev. B (to be published).

[5]D. C. Dahn and R. R. Haering, Solid State Commun. **44**, 29 (1982).

[6]W. R. McKinnon and J. R. Dahn, Solid State Commun. **52**, 245 (1984).

[7]J. R. Dahn and W. R. McKinnon, J. Electrochem. Soc. **131**, 1823 (1984).

[8]J. R. Dahn, M. A. Py, and R. R. Haering, Can. J. Phys. **60**, 307 (1982).

[9]W. R. McKinnon and R. R. Haering, *Modern Aspects of Electrochemistry*, edited by R. E. White, J. O. M. Bockris, and B. E. Conway (Plenum, New York, 1983), Vol. 15, p. 235.

[10]S. T. Coleman, W. R. McKinnon, and J. R. Dahn, Phys. Rev.

B **29**, 4147 (1984).

[11]G. Alefeld, G. Schaumann, J. Tretkowski, and J. Volkl, Phys. Rev. Lett. **22**, 697 (1969).

[12]G. Dolino, J. P. Bachheimer, B. Berge, C. M. E. Zeyen, G. Van Tendeloo, J. Van Landuyt, and S. Amelinckx, J. Phys. (Paris) **45**, 901 (1984).

[13]D. Durand, F. Denoyer, M. Lambert, L. Bernard, and R. Currat, J. Phys. (Paris) **43**, 149 (1982).

[14]K. Yvon, *Current Topics in Materials Science*, edited by E. Kaldis (North-Holland, Amsterdam, 1979), Vol. 3, p. 53.

[15]K. Yvon, R. Baillif, and R. Flukiger, Acta Crystallogr. Sect. B **35**, 2859 (1979).

[16]K. Yvon, R. Chevrel, and M. Sergent, Acta Crystallogr. Sect. B **36**, 685 (1980).

[17]H. Nohl, W. Klose, and O. K. Andersen, in *Superconductivity in Ternary Compounds I*, Vol. 32 of *Topics in Current Physics*, edited by O. Fischer and M. B. Maple (Springer, Berlin, 1982), p. 165.